Accepted Manuscript

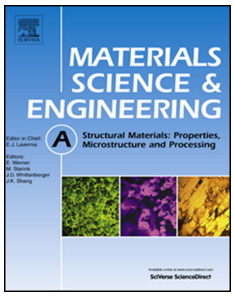

Direct-Quenched and tempered LOW-C high-strength structural steel: The role of chemical composition on microstructure and mechanical properties

Ari Saastamoinen, Antti Kaijalainen, Tun Tun Nyo, Dr Pasi Suikkanen, David Porter, Jukka Kömi

PII: S0921-5093(19)30783-X

DOI: https://doi.org/10.1016/j.msea.2019.06.018

Reference: MSA 38008

To appear in: *Materials Science & Engineering A*

Received Date: 13 April 2019

Revised Date: 4 June 2019

Accepted Date: 5 June 2019

Please cite this article as: A. Saastamoinen, A. Kaijalainen, T.T. Nyo, D.P. Suikkanen, D. Porter, J. Kömi, Direct-Quenched and tempered LOW-C high-strength structural steel: The role of chemical composition on microstructure and mechanical properties, *Materials Science & Engineering A* (2019), doi: https://doi.org/10.1016/j.msea.2019.06.018.

DIRECT-QUENCHED AND TEMPERED LOW-C HIGH-STRENGTH STRUCTURAL STEEL: THE ROLE OF CHEMICAL COMPOSITION ON MICROSTRUCTURE AND MECHANICAL PROPERTIES

M.Sc. Ari Saastamoinen, Dr. Antti Kaijalainen, B.Sc. Tun Tun Nyo, Dr. Pasi Suikkanen, Dr. David Porter, Dr. Jukka Kömi

ABSTRACT

The direct quenching of low-carbon steels after thermomechanical processing on hot strip mills is able to produce both strong and tough coiled plate without the need for subsequent tempering. The process is energy and time efficient with relatively low emissions when compared to conventional reheating, quenching and tempering. For some applications, however, it is desirable to combine direct quenching with tempering, and, bearing in mind the form of the semi-finished product, it is of interest to study the effect of tempering whole coils in a bell furnace. Here, the effects of boron, carbon, titanium, vanadium and tempering temperature on the microstructure, crystallography and mechanical properties of direct-quenched steels has been studied with the aid of simulated bell furnace heating and cooling cycles. All steels contained (in wt.%) 0.2Si-1Mn-1Cr-0.65Mo-0.03Al, while there were two levels of C (0.095 / 0.140), V (0 / 0.08), Ti (0 / 0.025) and B (0 / 0.0015). Tempering was performed with peak temperatures at 180 and 570 °C. The paper reveals several possible alloying and processing routes to strong and tough low-C steel. Carbon controls the strength and toughness, while titanium and boron affects the grain size of coarsest grains ($d_{90\%}$), Vanadium has a strong effect on strength retention during tempering at 570 °C: an addition of 0.08 wt.% vanadium increases yield strength by 70 MPa and ultimate tensile strength by 100 MPa. The removal of boron from the steel is shown to have a huge impact not only on the microstructure but also on the impact toughness.

KEYWORDS

Martensite, direct quenching, tempering, microstructure, high-strength, composition

1. INTRODUCTION

The metallurgy of re-austenitized and quenched (RAQ) martensite and re-austenitized, quenched and tempered (RAQT) martensite processing routes have been widely studied over many decades and is relatively well understood [1]–[5]. However, a similar understanding in the case alternative and recently developed direct-quenched and tempered (DQT) steels has yet to be achieved. Direct quenching (DQ) can provide remarkable improvements in both productivity and performance compared to traditional RAQ processing [6], [7]. Therefore, it is of interest to better understand the also the tempering metallurgy and properties of DQ steels.

As a further improvement for productivity in the case of direct-quenched coiled strip, a feasible, yet unreported tempering method is the batch annealing of full-scale steel coils. The tempering of coils in industrial bell furnaces would lead to significant improvements in productivity by allowing the tempering of large quantities of material in a single treatment. However, in addition to the development of a suitable production technology, an in-depth physical metallurgy analysis is not published and still required. Placing multiple steel coils in an industrial bell furnace creates its own

metallurgical demands due to the very slow heating and cooling rates.

The tempering of martensitic steels is generally divided into two separate processes: low-temperature tempering (LTT), i.e. heat treatment close to 200 °C, and high-temperature tempering (HTT) which usually is performed around 600 °C [1]. The temperature region in-between is often avoided due to embrittlement of martensite either due to segregation of impurities such as phosphorus and sulphur or because of the formation of cementite with an unfavourable shape and size [8]. The wide temperature gap between the two tempering processes means that various types of tempered microstructures are possible. In LTT, i.e. in temperature range of 150 – 200 °C, transition carbide formation has been reported to be the main microstructural change for martensitic steels [9]. However, for low-C steels (< 0.20C wt.%) formation of transition carbides is unlikely as due to autotempering, most of the carbon has already precipitated and no sufficient driving force exists in the structure for transition carbide formation. Therefore, mainly minor segregation of residual carbon and relief of residual stresses occur. [10] Carbon segregation lead to aging as carbon atoms lock free dislocations in the structure. Due to these reasons, tetragonality of low (less than 0.20 wt.%) carbon martensite is usually not seen due to auto-tempering during quenching [11]. LTT lath martensite in general has been reported to have very high hardness and strength, which is believed to correlate with the density of the transition carbides, carbon clustering and dislocations [1]. Dislocation densities have been shown to be carbon dependent [12] and are believed to control the strain hardening rate of LTT martensite leading to high strength and hardness [10].

For high-temperature tempered martensite, structural changes are more radical compared to tempering at lower temperatures. Potential transition carbides are first dissolved and then replaced with coarser cementite particles in addition to simultaneous dislocation densities decrease, leading to a drop in hardness [1], [11]. Alloy carbides may form [3] leading to secondary hardening. Traditional low-to-medium carbon RAQ martensite sees a significant improvement in toughness during high-temperature tempering [10]. However, the effect of tempering on the toughness of HTT direct-quenched steel has been shown to be complicated. Earlier, Kaijalainen et al. [13] and Pallaspuro et al. [14] studied the effect of high-temperature tempering on relatively low-alloyed DQ martensite. Their results showed that tempering improved the Charpy V 28 J transition temperature (T28J) especially for specimens orientated transverse to the rolling direction. By comparison, the toughness of RAQ martensite was seen to improve far more compared to DQ martensite. In the case of a somewhat more highly alloyed DQ martensite, the same research group showed that tempering did not improve toughness at all compared to the untempered DQ starting condition [14]. It should be noted though, that, in that case, yield strength was little affected by the tempering. These results indicate a probable compositional dependence of tempering on strength and toughness changes and they underline the need for a more detailed understanding of the effect of chemical composition on strength and toughness evolution during tempering.

Not always does the microstructure consist solely of martensite or tempered martensite. It is possible, for example, that in the case of limited hardenability martensitic-ferritic dual phase microstructures are formed during DQ. In such cases, it has been shown that tempering at 600 °C or below simply leads to the selective tempering of the martensitic regions while the ferritic regions remain largely unaffected [15], [16].

In HTT, titanium has been shown to be important for steels in terms of austenite grain growth behaviour, toughness and hardness evolution during tempering [17]–[22]. For re-austenitized and quenched martensite Shen et al. [20], [22] showed the importance of controlling the Ti/N ratio and the amount of titanium in excess of the stoichiometric amount with respect to N. In their study excess titanium lead to secondary hardening during HTT due to Ti(C,N) precipitation [20]. On the other hand, nitrogen in excess of the stoichiometric amount was found to lower hardenability and increase grain size. The optimal balance in terms of grain size and toughness was found with a

Ti/N ratio close to the stoichiometric 3.4. Similarly, Wang [18] noticed that the highest austenite grain coarsening temperature is reached with a stoichiometric Ti/N-ratio; any excess Ti leads to TiN precipitate coarsening and a reduced ability for the precipitates to retard grain coarsening. Similar preliminary findings were also made by the authors of this study for direct-quenched martensite [20]. Currently though, the similar study on the effect of titanium on tempering metallurgy of thermomechanical processed and direct-quenched steel is still lacking.

According to Bhadeshia and Honeycombe [11] even small V concentrations lead to the formation of very fine vanadium carbide platelets in martensitic steels tempered at 550 – 650 °C that may act as a secondary hardening elements. Pacyna and Dambrowski studied 0.33 - 0.35 wt.% C steels and showed that vanadium affects the start and finish temperatures for the formation of M_3C [23]. This means that, in addition to vanadium carbide precipitation, vanadium also seems to affect cementite growth behaviour. However, the effect of vanadium on direct-quenched martensite and especially for low-C steel is still not established in similar way.

Boron is known to strongly increase the hardenability of low-carbon steels [24]. However, under some circumstances, in direct-quenched lath martensite, a boron addition can lead to an increase of the effective grain size and a loss of toughness [25]. However, this is still not understood fully and the effect of tempering on B-free and B-alloyed direct-quenched martensite is still not studied. To fully understand the hardenability effect of boron, the effects of titanium and nitrogen need to be taken into account since titanium, as efficient nitride former, prevents boron from forming boron nitrides, which reduce the amount of boron in solid solution.

Carbon content plays a major role, not only with regard to hardenability, but also in controlling the strength of martensite [3]. Furthermore, carbon content will most likely affect the tempering kinetics of direct-quenched martensite through its effect on the driving forces for microstructural changes and softening. As low-C direct-quenched martensite is expected to undergo severe autotempering, it should be still studied whether the low-C autotempered martensite should be even tempered and how the variation of carbon content affects this.

In this study, it is the first time when slow heating and cooling conditions during tempering of direct-quenched steels are simulated in laboratory conditions. Furthermore, numerous potentially interesting chemical compositions are used to study long-term tempering resistance, i.e. ability to retain reasonable strength after long-term high-temperature tempering in this specific application. Therefore, the effect of V, C, B and Ti on tempering response of direct-quenched low-C with presumably martensitic microstructure are studied. No other study yet reports these in current application, which places totally new demands on the tempering resistance of martensitic matrix. In this way, the paper contributes to the better design of more energy-efficient production routes for future high-strength, high-toughness structural steels.

2. EXPERIMENTAL

Experimental steels

The experimental compositions shown in Table 1 were cast on the pilot scale with the aim of revealing the effects of carbon, vanadium, titanium and boron on the mechanical properties of direct-quenched steels prior to and after tempering. Pairwise comparison of the different compositions enables the individual effects of carbon, vanadium, titanium and boron to be determined for the 0.095C-0.2Si-1.0Mn-1.0Cr-0.65Mo-0.03Al base composition, see Fig. 1. Nitrogen content varied between 0.003 – 0.005 wt.%, leading to different levels of excess nitrogen.

The only exception to this was the titanium-microalloyed composition that has 0.016 wt.% titanium in excess of the stoichiometric amount required for the formation of TiN. Molybdenum was set to the level of 0.65 wt.% as it has been shown earlier to be essential in providing adequate tempering resistance [26].

Table 1. Chemical compositions of experimental steels (in wt.%).

Composition	C	Si	Mn	Cr	Mo	V	Ti	B	Al	N	S	O	M_s [27]
0.095C-0.08V-0Ti-15B	0.095	0.20	1.00	1.0	0.65	0.08	-	0.0015	0.030	0.004	0.006	0.004	465 °C
0.095C-0.08V-0.025Ti-15B	0.095	0.20	1.00	1.0	0.65	0.08	0.025	0.0015	0.030	0.003	0.003	0.002	465 °C
0.14C-0.08V-0Ti-15B	0.140	0.20	1.00	1.0	0.65	0.08	-	0.0015	0.030	0.003	0.003	0.002	446 °C
0.14C-0V-0Ti-15B	0.140	0.20	1.00	1.0	0.65	-	-	0.0015	0.030	0.003	0.006	0.004	446 °C
0.14C-0.08V-0Ti-0B	0.140	0.20	1.00	1.0	0.65	0.08	-	-	0.030	0.005	0.006	0.003	446 °C

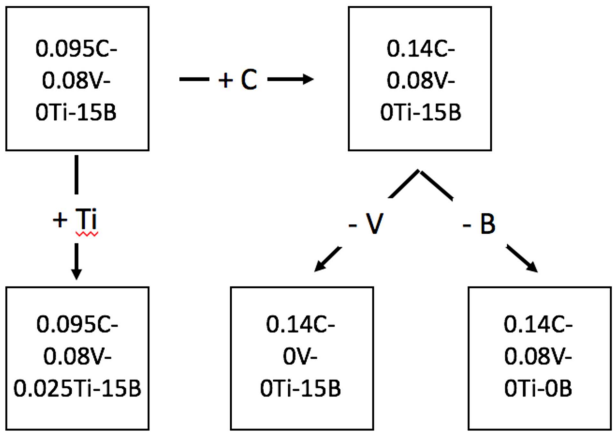

Fig. 1. Composition design.

Experimental slabs were hot rolled and directly quenched using a laboratory hot rolling mill. Based on the austenite grain growth studies described below, 55 mm thick slabs were reheated at 1225 °C for 2 hours. This was followed by hot rolling with 6 passes to a final plate thickness of 6 mm as detailed in Table 2. The estimated recrystallization stop temperatures were in the range of 880 – 890 °C and therefore the 5^{th} and 6^{th} rolling passes were performed below that temperature with the aim of obtaining pancaked austenite prior to direct quenching. Immediately after the final rolling pass at 800 °C the plate was directly quenched in a water bath at room temperature. The cooling rate during direct quenching measured with a thermocouple embedded in the middle of the slab prior to rolling was nearly 100 °C/s until approximately 400 - 450 °C from where the cooling rate started to slow down to 50 °C/s before reaching room temperature. The cooling curves were typical for direct quenched 6 mm thick steel using water quenching.

Table 2. Hot rolling schedule.

55 mm thick slab reheated at 1225 °C for 2 h			
Pass	Thickness (mm)	Temperature (°C)	Reduction (%)
1	43	1200	25
2	30	1150	36
3	21.5	950	28
4	14.7	910	32
5	9.6	860	35
6	6	800	38
Direct quenching into water tank with approximately 100 °C/s cooling rate			

Part of the direct-quenched material was subjected to both low-temperature tempering (LTT) and high-temperature tempering (HTT) using the thermal cycles given in Table 3, which were designed to simulate the slow heating and cooling rates experienced during the industrial tempering of large steel coils.

Table 3. Tempering parameters.

	Heating rate °C/min	Peak temperature °C	Soaking time min	Cooling rate °C/min
LTT	0.9	180	0	0.8
HTT	0.5	570	0	0.6

Microstructural evaluation

In order to reveal the austenite grain size after heating prior to rolling, as-cast slab material was heat treated for 2 h at 1225 °C and then quenched to a fully martensitic microstructure. Light optical microscopy on specimens etched in picric acid was then used to study the prior austenite grain morphology, and the prior austenite grain size distribution was determined using the mean linear intercept method. Equivalent circular diameter (ECD) as well as total reduction below the recrystallization temperature (R_{TOT}) and the austenite grain surface area per unit volume, S_V, (mm^2/mm^3) were also determined using the equations in Table 4.

Table 4. Equations used to calculate prior austenite grain size parameters [28].

Parameter	Equation
Aspect ratio, r	$r = {}^{L_{RD}}/_{L_{ND}}$
Total reduction, R_{tot} (%)	$R_{tot} = 1 - \sqrt{({}^{1}/_{r})}$
Surface area per unit volume (mm^2/mm^3)	$S_{v(g.b.)} = 0.429(N_L)_{RD} + 1.571(N_L)_{ND}$

L_{RD} is the mean linear intercept along RD, L_{ND} is the mean linear intercept along ND, r is the aspect ratio, R_{tot} is the total reduction below the recrystallization temperature, $S_{v(g.b.)}$ is the surface area per unit voluame and N_L is the number of grain boundary intercepts divided by lengths of lines along RD and ND respectively.

Direct-quenched steels were also investigated after picric acid etching to determine the prior austenite grain size and morphology after hot rolling and direct quenching. For some of the steels, it was very difficult to reveal the prior austenite grain size in this way, therefore the EBSD-based

method of Nyyssönen [29] was also used. In this method, an MTEX algorithm reveals the grain boundaries of the parent austenite based on the orientation relationship between martensite and the prior austenite.

Nital etching in combination with a Zeiss Sigma field emission scanning electron microscope (FESEM) equipped with an Inlens detector was used to study transformed microstructures after direct quenching and also to obtain high-resolution images of the carbides present before and after tempering. The Inlens secondary electron detector produces high-contrast images suitable for this purpose. Using ImageJ software grid analysis, the fraction of martensite and ferrite was determined. Furthermore, the effect of chemical composition on both low-angle and high-angle grain size and misorientation parameters at the quarter-thickness position of the HTT specimens was revealed with the aid of electron backscatter diffraction (EBSD) measurements combined with EDAX acquisition and analysis software. In the EBSD measurements, the FESEM was operated at 15 kV, the step size was 0.2 μm, and the total area analysed was 80 x 240 μm. Furthermore, the grain size at 90% in the cumulative grain area distribution was determined, as it has been earlier shown to correlate with impact transition temperature [28].

Semi-empherical CALPHAD approach of JMatPro® simulation software was used to predict the precipitates forming during tempering. It has been shown that for the tempering of martensite, JMatPro® predictions of precipitate types, fractions and radius correlate well with actual measured values in the tempering range of 200 – 700 °C and radius range of 0 – 0.4 μm [30], [31]. To compare the software simulations to actual carbide characteristics, TEM carbon replicas were prepared to study the shape and size of carbides after high-temperature tempering using a LEO 912 OMEGA Energy Filtered Transmission Electron Microscope (EFTEM).

Mechanical testing

Two tensile tests were carried out at room temperature for the DQ, DQ-LTT and DQ-HTT conditions in accordance with the European standard EN 10002 using flat specimens (6 x 20 x 120 mm^3) cut with their axes parallel to the rolling direction (RD). For specimens both parallel to and transverse to the RD, three 6-mm thick Charpy-V specimens were tested at each of six test temperatures from -140 to 0 °C in the DQ, DQ-LTT and DQ-HTT conditions according to the European standard EN 10045.

Tanh-fitting as described by Oldfield [32] using the procedure later introduced by EricksonKirk et al. [33] was used for defining Charpy V transition curves and determining both 28 J transition temperatures and 95 % confidence intervals. To convert sub-sized T28J values to their full-size equivalents, the method presented by Wallin [34], [35] was used.

3. RESULTS

Slab reheating

Table 5 shows the effect of chemical composition on austenite grain size after slab reheating treatments. In one case, abnormal grain growth was observed and this is indicated by an asterisk in the table. In this case, the grain size given is that excluding the abnormally large grains, i.e. the "matrix" grain size. Most of the compositions result in homogeneous grain sizes in the range 130 - 190 μm. In the case of the composition microalloyed with Ti (0.95C-0.08V-0.025Ti-15B), the matrix grain size is much smaller than in the corresponding Ti-free composition (0.95C-0.08V-0Ti-

15B), staying below 50 μm, but abnormal grain growth results in the occurrence of very large grains after heating, see Fig. 2.

Table 5. Mean reheated austenite matrix grain sizes with 95 % confidence intervals after slab reheating with a 120 min holding time at 1225 °C.

Composition	Matrix grain size (μm)
0.095C-0.08V-0Ti-15B	132 ± 19
0.095C-0.08V-0.025Ti-15B	44 * ± 3
0.14C-0.08V-0Ti-15B	189 ± 26
0.14C-0V-0Ti-15B	183 ± 26
0.14C-0.08V-0Ti-0B	157 ± 20

* Bimodal grain structure including coarse grains in fine matrix (size of the smaller, matrix grains given)

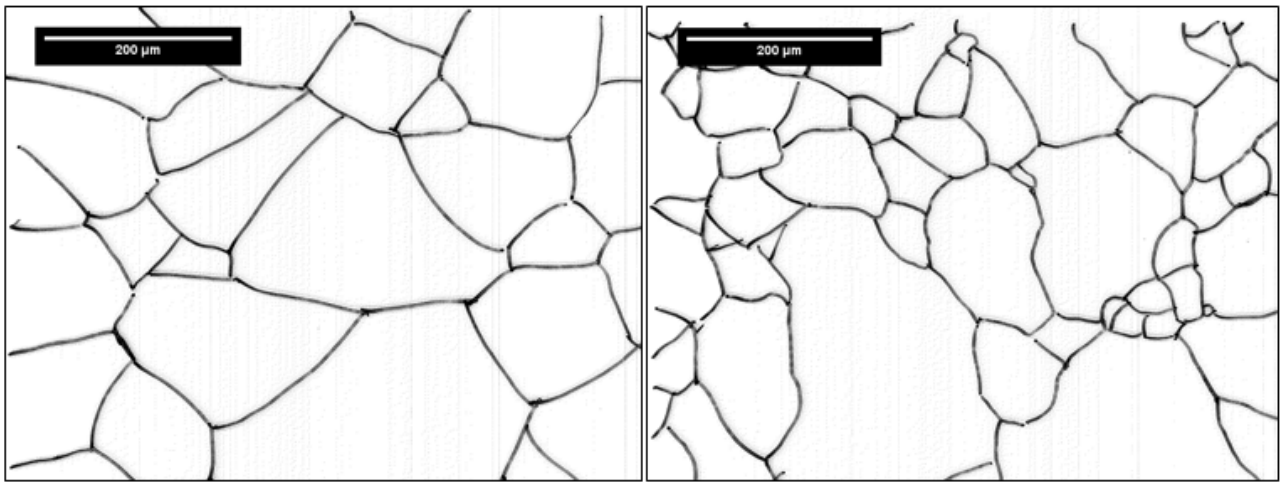

Fig. 2. Austenite grain structure after slab annealing at 1225 ˚C for 2 hours in (a) Ti-free and (b) Ti-alloyed composition . Reprocessed after light optical microscope and picric acid etching for better grain boundary quality.

Microstructure of hot-rolled materials

Fig. 3 and Table 6 show the differences in the prior austenite grain morphologies after hot rolling. Despite the presence of some abnormal grain growth in the Ti-alloyed composition prior to hot rolling, the as-rolled prior austenite grain structure (Fig. 3b) is significantly finer than the corresponding composition without Ti (Fig. 3a). As seen in Table 6, the only significantly different grain structure is that obtained with the Ti-alloying concept, which provided the finest prior austenite grain size. The other compositions gave similar prior austenite grain structures. The B-free steel had a slightly more equiaxed grain structure as witnessed by the lowest values of the grain aspect ratio, r, and the total reduction below the recrystallization temperature, R_{TOT}.

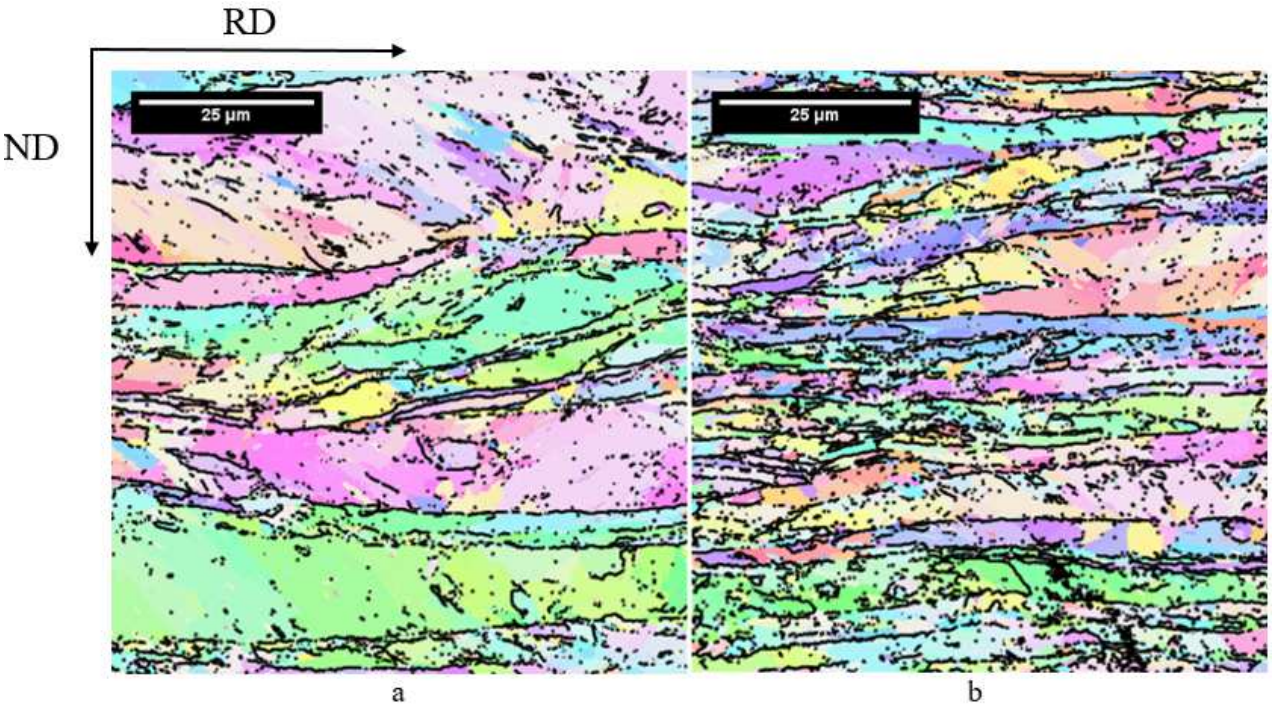

Fig. 3. Prior austenite grain boundaries revealed using Nyyssönen's [28] method after slab reheating, hot rolling and direct quenching. Prior austenite grain structures of (a) Ti-free steel 0.095C-0.08V-0Ti-15B and (b) Ti-alloyed steel 0.095C-0.08V-0.025Ti-15B show the significant influence of Ti during TMCP+DQ processing.

Table 6. Prior austenite grain size parameters in the direct-quenched condition.

Composition	PAGS, ECD (µm)	R_{tot} (%)	r	$S_{v(g.b.)}$ (mm^2/mm^3)
0.095C-0.08V-0Ti-15B	18.8	62	7.0	235
0.095C-0.08V-0.025Ti-15B	8.9	64	7.6	505
0.14C-0.08V-0Ti-15B	22.3	59	6.0	183
0.14C-0V-0Ti-15B	17.3	62	6.9	251
0.14C-0.08V-0Ti-0B	18.6	54	4.7	193

Fig. 4 shows FESEM Inlens images of the materials in the hot-rolled and direct-quenched condition after etching with nital. The main microstructural component is autotempered martensite. However, in addition to autotempered and some amount of fresh martensite, it can be seen that the hardenability of the base composition is insufficient to produce a fully martensitic microstructure under the present rolling and cooling conditions: polygonal ferrite is clearly seen. Raising C to 0.14 wt.% increases the hardenability such that the microstructure is then fully martensitic. Similarly, the addition of Ti to the base composition improves the hardenability to the extent that only a small fraction of fine polygonal ferrite can be seen. This is presumably due to the well-known influence of Ti in protecting B against reaction with N by the formation of stable TiN precipitates [36]. Also, excess Ti has been shown to improve hardenability [20]. Fig. 4 shows that the removal of V from the higher C composition also results in the appearance of polygonal ferrite, but that the removal of boron results in a greater loss of hardenability and more ferrite in the final microstructure. In fact the B-free steel contained 12 % ferrite. Table 7 presents the martensite and ferrite volume fractions

evaluated from the FESEM Inlens images using ImageJ grid analyses. It also shows the calculated carbon contents of ferrite and martensite based on calculations using 0.025 wt.% carbon solubility in the ferrite.

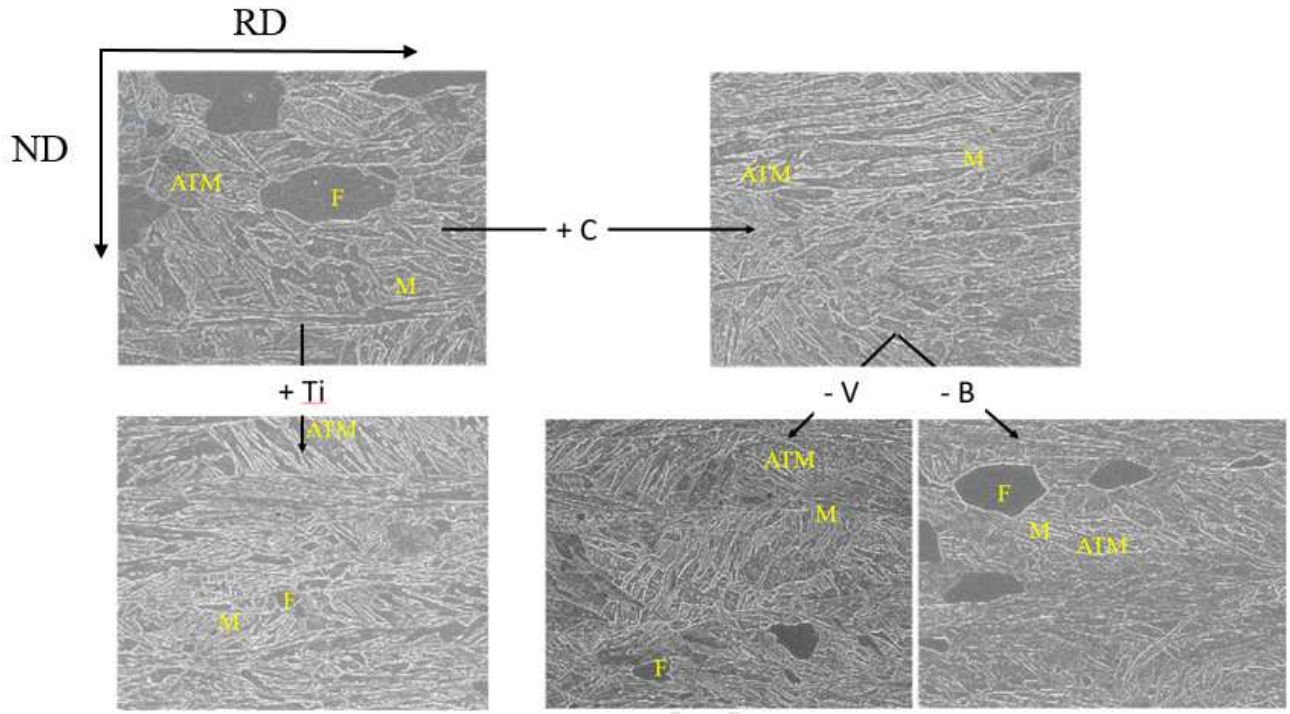

Fig. 4. FESEM Inlens images of DQ conditions at the quarter-thickness of the strip. Ferrite (F), martensite (M) and autotempered martensite (ATM) are presented in the figure.

Table 7. Martensite and ferrite volume fractions determined from FESEM-Inlens images and calculated carbon content of martensite.

Composition	Martensite volume fraction	Ferrite volume fraction	C_m wt.%
0.095C-0.08V-0Ti-15B	0.89	0.11	0.110
0.095C-0.08V-0.025Ti-15B	0.94	0.06	0.099
0.14C-0.08V-0Ti-15B	1.00	0.00	0.140
0.14C-0V-0Ti-15B	0.96	0.04	0.150
0.14C-0.08V-0Ti-0B	0.88	0.12	0.160

One might expect differences between the two carbon contents in terms of autotempering given the effect of carbon on martensite start temperature and ultimately the autotempering kinetics. However, when comparing the appearance of the carbides in the autotempered martensite, no obvious differences are apparent irrespective of whether the carbon content is 0.095 % (Fig. 5a, 0.095C-0.08V-0Ti-15B) or 0.14 % (Fig. 5b, 0.014C-0.08V-0Ti-15B). This is presumably due to the fact that the two bulk carbon contents do not differ much from each other and the fact that, due to the formation of polygonal ferrite, the carbon content of the martensite in the lower carbon steel will be somewhat higher than the bulk, as shown in Table 7.

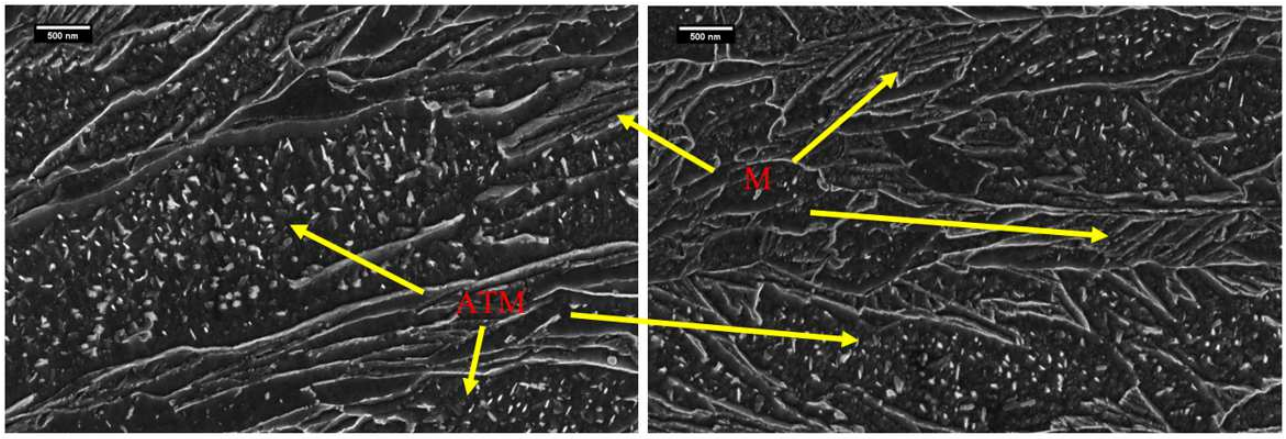

a b

Fig. 5. FESEM-Inlens images of (a) 0.095C-0.08V-0Ti-15B and (b) 0.014C-0.08V-0Ti-15B experimental steels in the direct-quenched conditions. Both carbon contents lead to severe autotempering.

Similar microstructural characterization was also performed for the DQ-LTT conditions, see Fig. 6. No major differences between the DQ-LTT and DQ conditions are apparent with the resolution of FESEM: autotempered or tempered martensite is the main microstructural component in both as the carbon clustering is expected to be main microstructural change in the procedure.

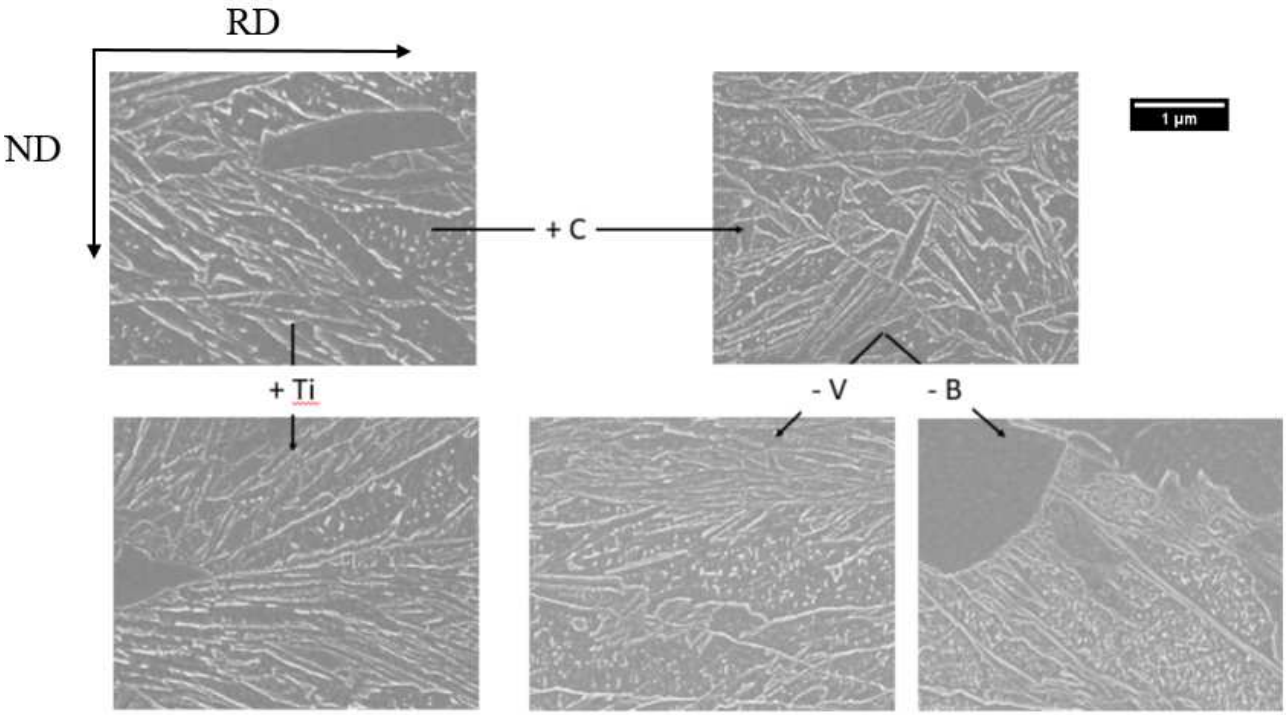

Fig. 6. FE-SEM Inlens images in DQ-LTT conditions at the quarter-thickness of the strip. Microstructure consists of tempered martensite in addition to some polygonal ferrite.

During the long high-temperature tempering treatment to the high peak temperature of 570 °C, all the studied steels undergo strong carbide coarsening, as shown in Fig. 7. TEM extraction replica studies showed that the carbides are Fe_3C, see Fig. 8. Typically, carbides reach size up to 200 nm in length and approximately 50 nm in width. Despite the long high-temperature tempering procedure, the spheroidization process is incomplete, leaving the carbides elliptical in shape with lengths up to

200 nm and widths up to 50 nm. In the Ti microalloyed steel, small TiN precipitates are also seen in the extraction replicas as shown in Fig. 8.

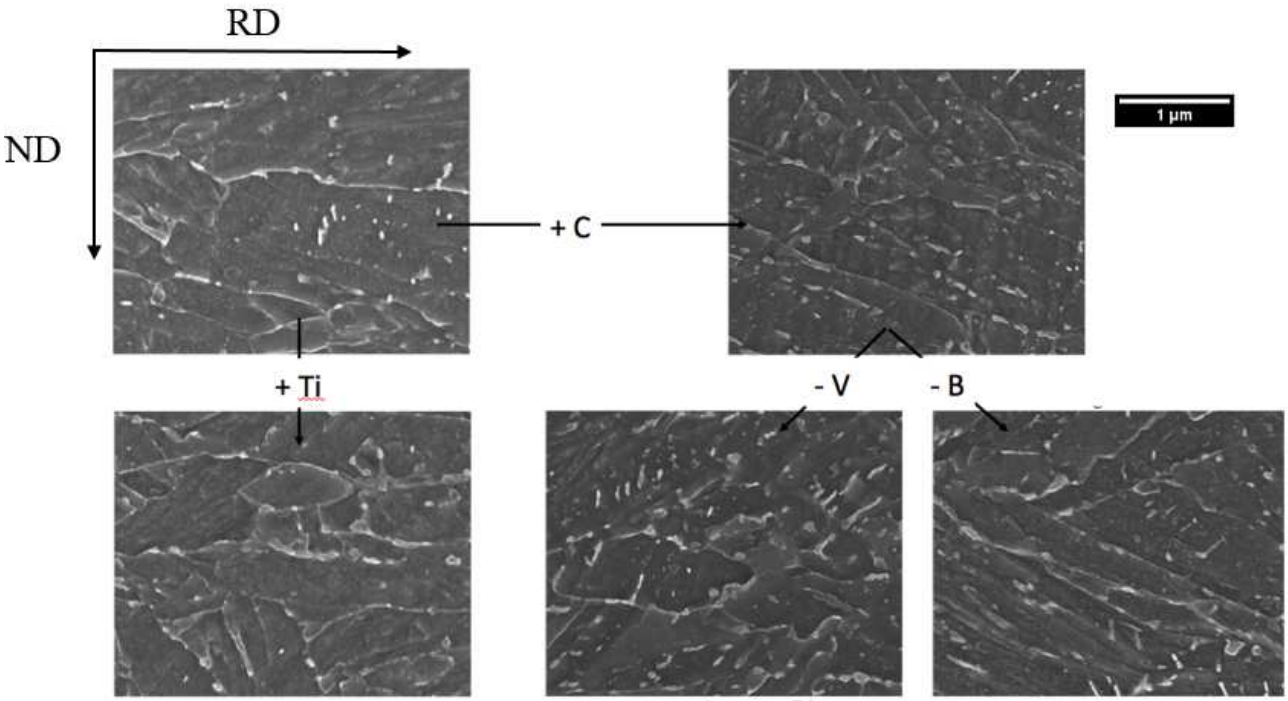

Fig. 7. FESEM Inlens images in DQ-HTT conditions showing the effect of composition on tempered microstructure.

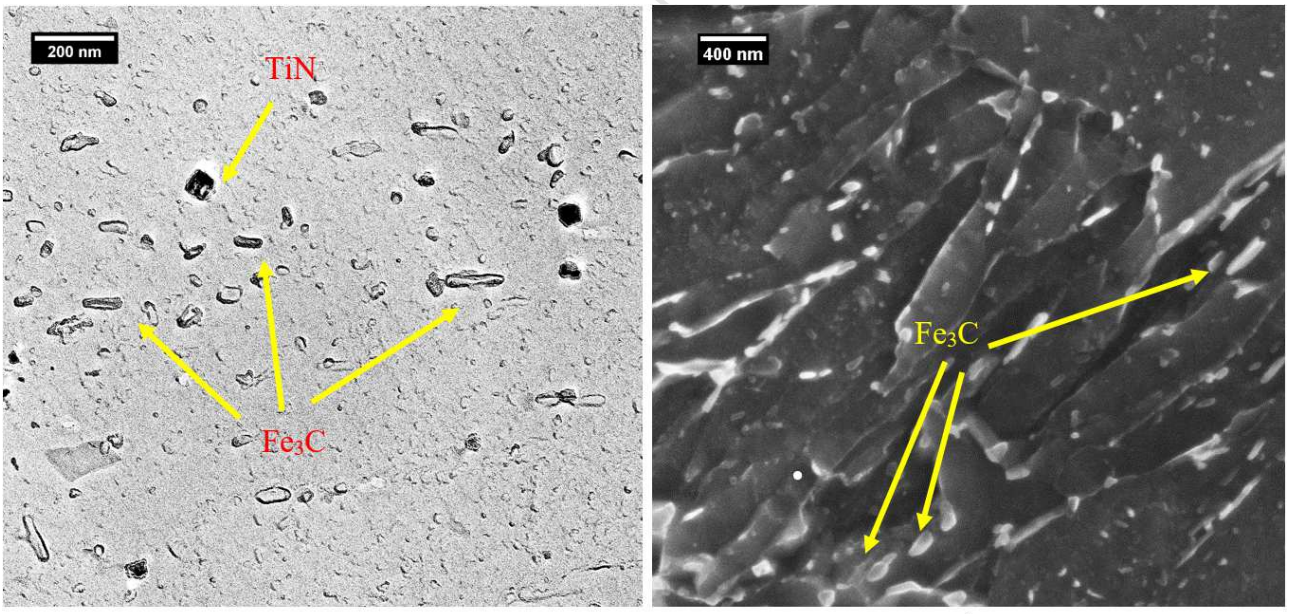

a b

Fig. 8. 0.095C-0.08V-0.025Ti-15B in the HTT condition. (a) TEM carbon extraction replica images and (c) FESEM-Inlens image. Coarse cementite is dominant precipitate in the structure.

The results of the microstructural characterizations are generally in line with the predictions of the JMatPro® software, which, for the current compositions and HTT conditions, predicts the precipitation of two main carbides during the tempering of martensite: 1) M_3C with a radius of 100-120 nm and volume fraction of 1.1 %, and 2) M_7C_3 with a radius of 25 nm and volume fraction of 0.5 %, see Fig. 9. The differences in the chemical compositions of the steels do not have much influence on the predictions. It is valuable though that the TEM and FESEM images show that the

sizes of coarser carbides, i.e. cementite, are generally roughly in the same scale than predicted by the JMatPro software.

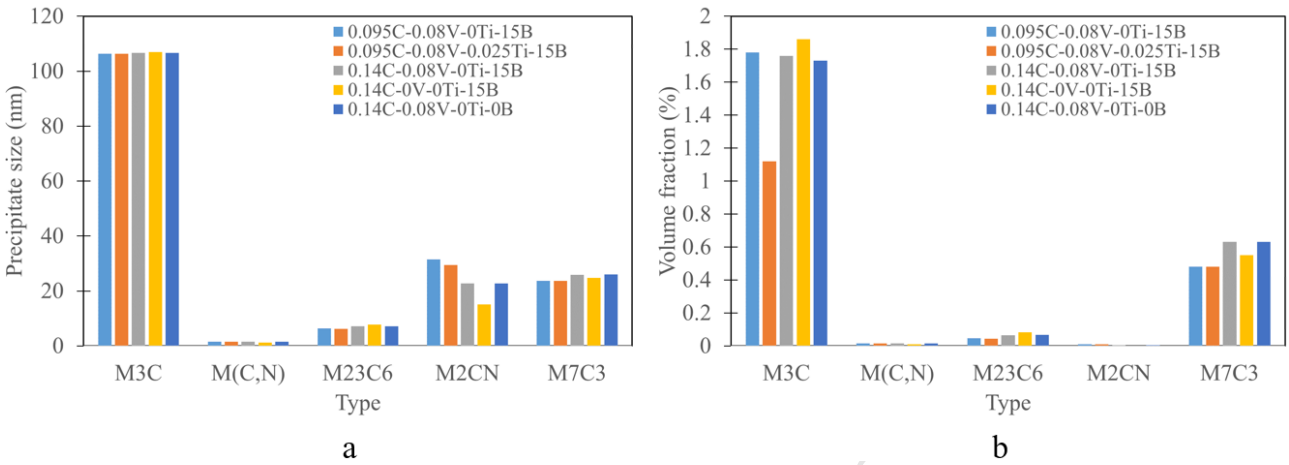

Fig. 9. Predicted carbide radius (a) and volume fractions (b).

For the HTT condition, the EBSD data was also used to determine the mean sizes of grains by low-angle (>2°) and high-angle (>15°) boundaries expressed as equivalent circle diameters (ECD). On the basis of earlier results that showed that there are no significant differences in grain size and texture between the DQ and HTT (570 °C) conditions [14], only the HTT condition was studied here. In addition to low- and high-angle grain sizes, the ECD value of the 90th percentile in the cumulative grain area distribution ($d_{90\%}$) was determined. The effect of chemical composition on grain size parameters is presented in Fig. 10. As far as the mean low- and high-angle grain sizes are concerned, there seem to be no differences between the steels. However, chemical composition has an influence on $d_{90\%}$: the presence of Ti significantly refines the size of the coarsest grains, i.e. $d_{90\%}$, by 37 %, which is visible also in the EBSD IPF maps (Fig. 11). EBSD maps also show the heterogeneity of the grain structure. The microstructure of the low-carbon Ti-free steel also contained coarse polygonal ferrite and, as can be seen in Fig. 4, the polygonal ferrite has a coarse grain size, which presumably also affects the higher $d_{90\%}$ of the partly ferritic low-C steel. The boron-containing steels with higher carbon, on the other hand, provided fully martensitic steel with a larger size of the coarsest grains. Vanadium did not have an effect on grain size despite slightly improving the hardenability of the composition.

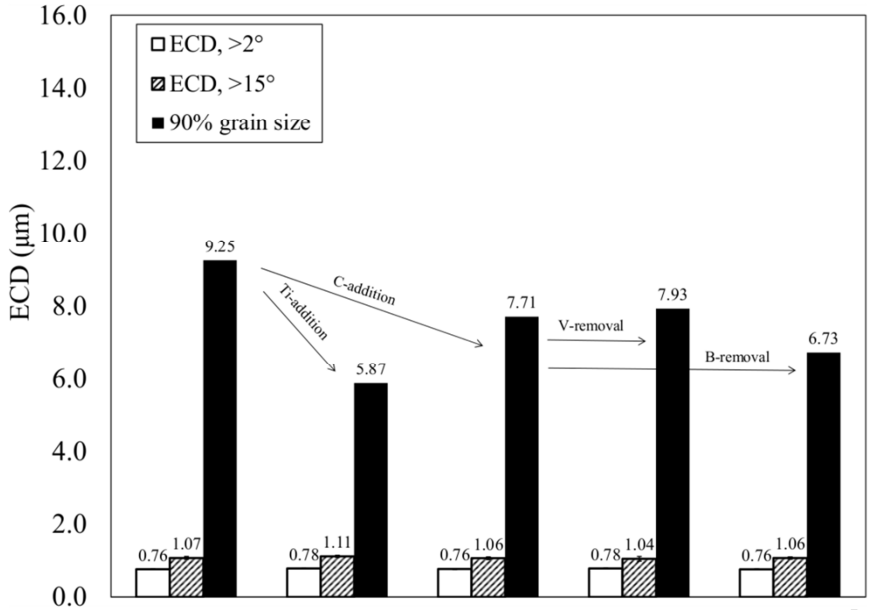

Fig. 10. Grain sizes for the HTT conditions. Mean ECD values for grains surrounded by low-angle and high-angle boundaries together with cumulative 90th percentile ECD values for grains surrounded by high-angle boundaries ($d_{90\%}$).

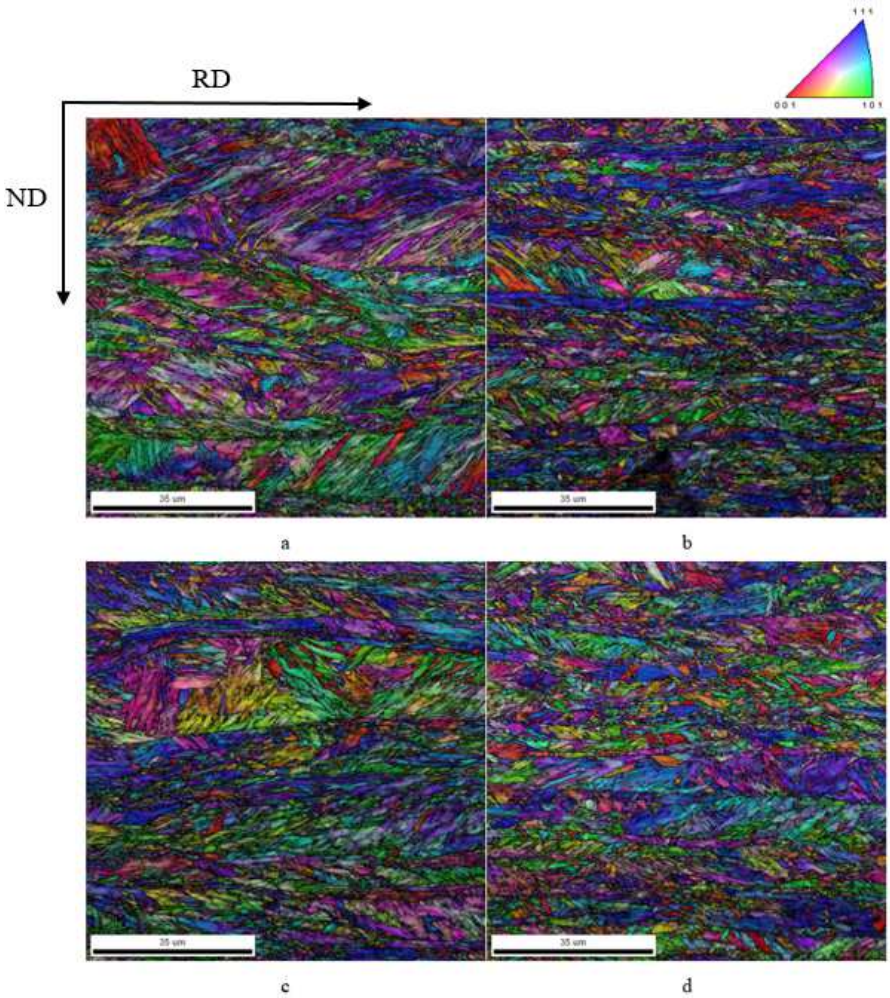

Fig. 11. EBSD inverse pole for (a) 0.095C-0.08V-0Ti-15B and (b) 0.095C-0.08V-0.025Ti-15B, (c) 0.14C-0.08V-0Ti-15B and (d) 0.14C-0.08V-0Ti-0B steels at HTT condition. Black grain boundary

lines show high-angle boundaries (> 15°). Ti-alloyed and B-free compositions show finest microstructures of the study.

Mechanical properties

Table 8 shows the tensile properties and Charpy V 28 J transition temperatures in the DQ condition and after tempering at low and high temperatures. Direct-quenched strength values are generally well in line with the varying ferrite and carbon contents: the B-free steel with 12 % ferrite shows low strength despite its higher carbon content and both the V- and B-alloyed 0.14C steels show the highest strengths. It can also be seen that vanadium reduces the softening of the direct-quenched strip steel resulting from HTT. The alloying of only 0.08 % V leads to a 100 MPa difference in tensile strength and a 70 MPa difference in yield strength after HTT despite similar yield and tensile strengths in the direct-quenched condition. Softening also leads to increased toughness; the V-alloyed composition with the higher UTS has almost a 50 °C higher 28J transition temperature (T28J) compared to V-free counterpart. Interestingly, these differences are not visible in the low-temperature tempered condition. Furthermore, the V-free steel is the only one where high-temperature tempering improves T28J.

The composition possessing high carbon content together with vanadium and boron showed the lowest toughness for all processing conditions. Especially after high-temperature tempering, the 0.14C-0.08V-0Ti-15B steel obtained very poor toughness (T28J) compared to the other steels. The transition curves fitted with procedure mentioned above are presented in Fig. 12. Generally, transition curves of DQ and DQ-LTT materials are very similar regardless of increase in yield strength after low-temperature tempering. High-temperature tempering on the other hand increases upper shelf energy by 20 – 30 J despite no decrease in yield strength and no improvement in 28J transition temperature. These results also show that removal of either boron or vanadium lowers T28J. Also, surprisingly, removing Ti from the composition leads to an improved toughness despite the fact that tis results in a coarser effective grain size ($d_{90\%}$).

The low-temperature tempered conditions had higher yield strengths than the direct-quenched conditions, though ultimate tensile strength was retained at nearly the initial level. What is the most noticeable result, is the fact that for all compositions toughness, as measured by T28J, was impaired by the low-temperature tempering.

Table 8. Mean yield strength (YS), ultimate tensile strength (UTS), total elongation, uniform elongation and 28J transition temperatures including 95% confidence intervals. Yield strength (YS) refers to the stress for 0.2% plastic strain.

	YS (MPa)	UTS (MPa)	Elongation (%)	Uniform elongation (%)	T28J Long (°C)
DQ					
0.095C-0.08V-0Ti-15B	908 ± 13	1226 ± 9	12.1 ± 0.4	5.0 ± 0.1	-103 (-130…-92)
0.095C-0.08V-0.025Ti-15B	953 ± 0	1264 ± 8	12.5 ± 1.5	4.7 ± 0.1	-74 (-106…-60)
0.14C-0.08V-0Ti-15B	1011 ± 0	1404 ± 8	11.4 ± 0.4	4.8 ± 0.4	-50 (-75…-26)
0.14C-0V-0Ti-15B	1000 ± 15	1384 ± 9	11.8 ± 1.7	4.8 ± 0.2	-56 (-68…-45)
0.14C-0.08V-0Ti-0B	968 ± 28	1351 ± 48	12.1 ± 1.5	4.7 ± 0.8	-98 (-132…-52)
DQ-T 180 °C (LTT)					
0.095C-0.08V-0Ti-15B	1027 ± 9	1237 ± 11	11.1 ± 1.2	3.9 ± 0.1	-76 (-99…-53)
0.095C-0.08V-0.025Ti-15B	1051 ± 9	1247 ± 11	11.5 ± 0.1	3.7 ± 0.2	-65 (-84…-46)
0.14C-0.08V-0Ti-15B	1113 ± 8	1387 ± 4	11.2 ± 0.2	3.8 ± 0.2	-36 (-53…-20)
0.14C-0V-0Ti-15B	1093 ± 21	1377 ± 3	11.4 ± 1.7	4.2 ± 0.4	-39 (-58…-38)
0.14C-0.08V-0Ti-0B	1044 ± 8	1310 ± 22	11.7 ± 0.2	4.2 ± 0.3	-73 (-88…-58)
DQ-T 570 °C (HTT)					
0.095C-0.08V-0Ti-15B	1027 ± 17	1081 ± 12	15.9 ± 0.9	5.4 ± 0.7	-79 (-105…-54)
0.095C-0.08V-0.025Ti-15B	1085 ± 1	1128 ± 6	16.3 ± 1.0	5.2 ± 0.7	-54 (-75…-33)
0.14C-0.08V-0Ti-15B	1093 ± 2	1163 ± 2	13.7 ± 1.1	4.7 ± 0	-33 (-59…-7)
0.14C-0V-0Ti-15B	1021 ± 24	1063 ± 25	15.3 ± 1.1	5.6 ± 0.1	-80 (-96…-65)
0.14C-0.08V-0Ti-0B	1036 ± 47	1112 ± 30	14.4 ± 0.3	5.4 ± 0.1	-60 (-84…-38)

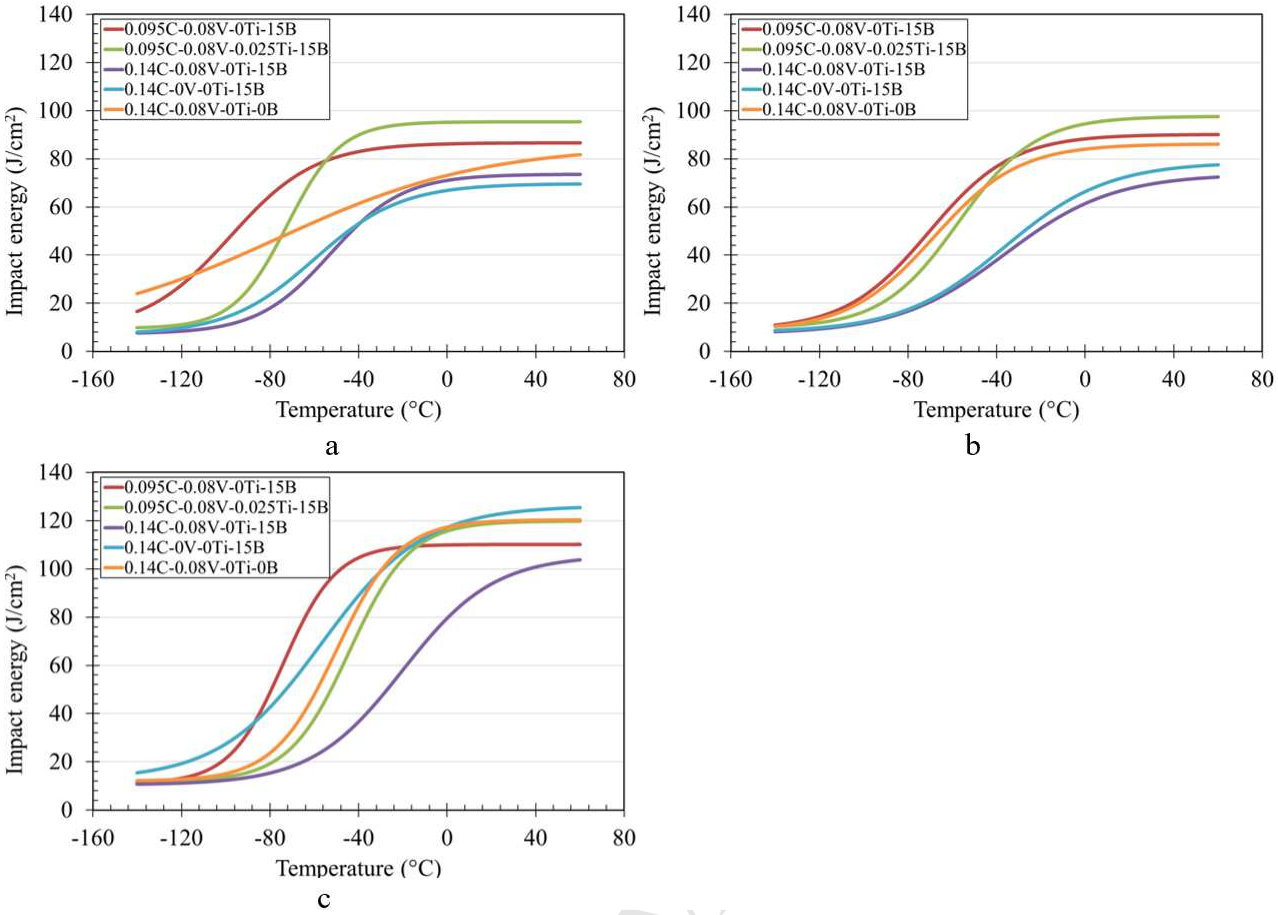

Fig. 12. Charpy V transition curves for the (a) DQ, (b) LTT and (c) HTT conditions. Fitted curves are determined by the method of Oldfield and EricksonKirk [32], [33]**.**

4. DISCUSSION

Results of this study show the importance of chemical composition on both initial austenite grain size, transformed microstructures and, importantly, tempering resistance of ultra-slowly tempered direct-quenched steels.

Titanium had a significant effect on the initial austenite grain size and refined the grain size of annealed slab, which is in line with observations in earlier research regarding the effects of Ti and TiN precipitates on austenite grain size and grain coarsening temperature [37]–[39]. However, earlier studies also share the understanding that the highest austenite grain coarsening temperature can be obtained with a Ti/N ratio close to the stoichiometric value of 3.42. Therefore, the current Ti-alloyed composition with a Ti/N ratio of 9.3 giving 0.015 wt.% excess titanium is not the optimum as regards grain size control and most likely lead to unnecessary coarsening of titanium nitrides. However, the result again shows the effectiveness of Ti even when Ti/N is not the optimal. Despite the presence of some abnormal grain growth in the Ti-alloyed composition prior to hot rolling, the as-rolled prior austenite grain structure (Fig. 2b) is significantly finer than the corresponding composition without Ti (Fig. 2a). Furthermore, the size of the coarsest grains in the final steel HTT microstructures ($d_{90\%}$) was finer for the Ti-alloyed steel, which again is presumably due to the inhibition of grain growth by TiN prior and during hot rolling, ie. interpass recrystallization, despite the fact that a finer precipitate size resulting from a composition closer to the stoichiometric ratio would probably have promoted refinement even more [40]. All but one of

the steels contain 0.08 wt.% V, but because vanadium carbonitride precipitates dissolve in austenite at relatively low temperatures the vanadium microalloying had little effect on austenite grain size at typical slab reheating temperatures as also noted by Kobayashi [41].

The amount of nitrogen in the Ti-alloyed composition was 27 ppm giving 150 ppm Ti in excess of that required to form TiN, which leads to increased hardenability due to the boron protection effect [18], [20]. However, excess Ti over stoichiometric Ti/N-ratio did not improve tempering resistance in the current study as much as was expected based on our earlier results [20] and only a small increment in HTT strength was obtained with Ti-addition from Ti-free condition. However, despite of its effective grain refinement effect, excess Ti is detrimental to impact toughness in all tempering conditions (Fig. 14a). The same effect has been observed earlier by the present authors [20] and by Yan et al. [17] who observed a decrease in toughness with increasing Ti/N-ratio over stoichiometric due to the coarsening of TiN particles.

The effect of boron can be discussed from two separate points of view – toughness and strength. As microstructural characterization revealed, the absence of boron leads to the formation of ferrite prior to the formation of martensite and also lower initial strengths. The results show that boron increased hardenability despite the absence of titanium protection. The lower strength of the partly ferritic steel is understandable, but it does not explain the great difference in toughness between the B-free and B-alloyed composition (Fig. 14c). DQ, and DQ-LTT and DQ-HTT B-free steels have an almost 50 °C lower T28J than their B-alloyed counterparts, which seems remarkable considering the relatively minor difference in strength. The results in this study however indicate that the removal of boron leads to a refinement of both prior austenite grain size and the effective coarse grain size $d_{90\%}$. Furthermore, removing boron leads to a smaller ECD for the PAGS and a higher S_V (mm^2/mm^3), which has been shown to correlate positively with impact toughness [42]. Hannula et al. [25] have reported a similar effect of B on the toughness of DQ steels. The mechanism leading to a finer effective coarse grain size $d_{90\%}$ accompanying the removal of B is unclear. In the results presented above, the B-free partly ferritic steel obtained a finer $d_{90\%}$ grain size compared to the B-alloyed fully martensitic steel. However, the low-C steel, which was also partly ferritic, obtained a coarser $d_{90\%}$ grain size than the higher carbon steel that had a fully martensitic microstructure. Therefore, no definite conclusion can be made regarding the effect of ferritic regions on the effective grain size of direct quenched steel. Regardless, the $d_{90\%}$ grain size has been shown to be an important factor affecting the toughness of DQ steels [7],[28]. On the refining effect of B removal on grain size, Gao et al. [44] made similar findings and proposed that austenite grain size increases with increased boron content due to the formation of BN, which reduces the amount of grain refining AlN. Pallaspuro et al. [43] showed the importance of grain refinement and a correlation between toughness and martensite content for martensitic-bainitic high-strength steels, where an almost linear decrease in toughness with increasing martensite content was found. However, the results of the current study concern martensitic-ferritic steels instead of martensitic-bainitic steels. In fact, some studies on dual phase martensitic-ferritic steels have been made with focus on the effect of a large fraction of martensite. Bag et al. [45] studied the effect of martensite content between 33 – 62 % and found a strong increase in toughness with increasing martensite content. However, there are no earlier studies concerning the toughness of martensitic - ferritic steels with low ferrite fractions.

The role of carbon content on the ultimate tensile strength of re-austenized and quenched martensite has been studied widely in the past [3]. This study show (Fig. 13d) the expected result that carbon content is the main factor controlling ultimate tensile strength also in the case of direct-quenched martensitic-ferritic steels. However, in the current study, the increase in carbon content leads to the combined effect of both removing ferrite (Fig. 4) and increasing martensite strength. In fact, the formation of ferrite also pushes carbon into the austenite and therefore increases the carbon content

of the untransformed austenite, which subsequently transforms to martensite with a higher carbon content and strength. Titanium and boron also affected the UTS of the direct-quenched condition. This again can be explained by their effects on the presence of the softer ferrite component. Furthermore, The B-free steel has higher carbon content (0.14 wt.%) but still contains 12 % ferrite. This raises the carbon content of the martensite even further making the carbon content of the martensite in the M-F microstructure of the B-free composition the highest of all the steels that in theory should reduce the amount of autotempering and decrease the ductility in as-quenched condition.

Due to low carbon content of the steel, transition carbide precipitation is unlikely in low-temperature tempering due to autotempering and main microstructural change occur at very small scale as relief of residual stresses and clustering of residual carbon and locking of free dislocations are expected to occur. This phenomena, also known as, aging static strain aging is expected to be reason behind promoting yield strength of LTT conditions. [3], [10], [11]

For all conditions studied, lowering the carbon content from 0.14 to 0.095 % lowers the transition temperature by 50 °C, see Fig. 14d. A similar finding regarding the effect of carbon on toughness has been reported by Suikkanen et al. [46] for TRIP-aided ultra-high-strength steels as well as by Krauss for RAQ and RAQT martensitic 43xx steels [2]. This carbon dependent toughness behaviour is believed to be due to an increase of internal stresses with increasing carbon content. Hutchinson et al. [47] showed that short-range microstresses may be the cause of the relatively low yield strength of as-quenched martensite compared to low-temperature tempered martensite [48]. However, an improvement in T28J is not obtained with either LTT or HTT. Higher carbon content also leads to increased strain hardening see Fig. 13d. Undoubtedly, the effect of carbon content on internal stresses and their behaviour on tempering is a matter requiring further studies.

The effect of increased strength due to higher carbon content is reduced as a result of tempering (Fig. 13d). In the direct-quenched condition, the UTS of the 0.14%C B-alloyed composition was 178 MPa higher than that of the 0.095%C B-alloyed composition, but in the HTT condition the difference was only 82 MPa. This is understandable as earlier results show the carbon content dependence of hardness, dislocation density and residual stresses in the structure [3], [12]. As tempering progresses, carbon in solution in martensite precipitates as cementite, leading to a lower carbon content in martensite and ultimately lower tensile strength.

Results presented above show that by modification of chemical composition, significant improvement can be obtained in retaining strength after tempering. Vanadium addition promotes the tempering resistance remarkably and lead to even increased yield strength after high-temperature tempering despite demanding long tempering procedure that was performed to simulate the industrial bell furnace treatment. Demand of robust steel composition is even higher when we consider the temperature gradients in tight coil annealing as described by Harvey. [49] So-called cold spot and hot spots in the coil can differ even 30 – 40 °C leading to potentially strength gradients in tempered condition of the strip, which can be even further promoted by poor composition design.

Vanadium is a strong carbide and carbonitride former and is used for precipitation strengthening during tempering [11], [50]. It has been noticed that even small additions of vanadium can form V_4C_3 or VC carbides at the tempering temperatures of 550-650 °C, leading to secondary hardening [11]. However, these earlier results show that the size of these precipitates is extremely fine, less than 10 nm. Whether or not such precipitates were present in the present steels could not be determined on the basis of the extraction replicas. Lagneborg et al. [50] have shown that VN precipitates are also effective at increasing strength albeit at the expense of toughness. Such

strengthening requires nitrogen levels in the range of 50 to 200 ppm, i.e. more than that in the current steels., and no VN particles were found in the extraction replicas either. It should be noted also that processing route in their study is different and do not cover tempering of direct-quenched strip. However, Gündüz et al. [51], showed that tempering of 0.10% V steel at 600 °C produced a clear secondary hardening effect due to the formation of closely spaced precipitates. Regardless of low nitrogen levels (30 – 40 ppm), the results in our study show that vanadium addition also retards softening for direct-quenched steels during HTT at significant rate (Fig. 13b). The V-free steel softened significantly as a result of HTT and in addition to softening, a remarkable increase in toughness occurred for the V-free steel during tempering (Fig. 14b). In fact, the V-free steel was the only experimental steel that showed an increase in toughness during either LTT or HTT compared to the initial situation. The better impact toughness of the V-free composition compared to the V-alloyed steel, might be due to formation of these very fine VC and/or V_4C_3 carbides that effectively increase strength but reduce toughness. In addition to tempering resistance in terms of tensile strength, the yield strength of the V-alloyed steel also increased at a higher rate during the tempering compared to V-free steel in both the LTT and HTT, which indicates the presence of precipitate strengthening. V-free steels also had minor amount of ferrite in the structure while V-alloyed counterpart obtained fully martensitic microstructure. Earlier, vanadium microalloying has been shown to retard the formation of protectoid ferrite. [52]. Furthermore, this hardenability increasing effect of vanadium should be considered through other microalloying elemens and titanium contents as according to Adrian [53] free nitrogen will lead to formation of vanadium nitrides and therefore solely adding vanadium into solution is not likely to improve hardenability itself. Adrian presented that microalloying of titanium, aluminium or zirconium will promote hardenability effect of vanadium. Especially efficient of these elements was titanium.

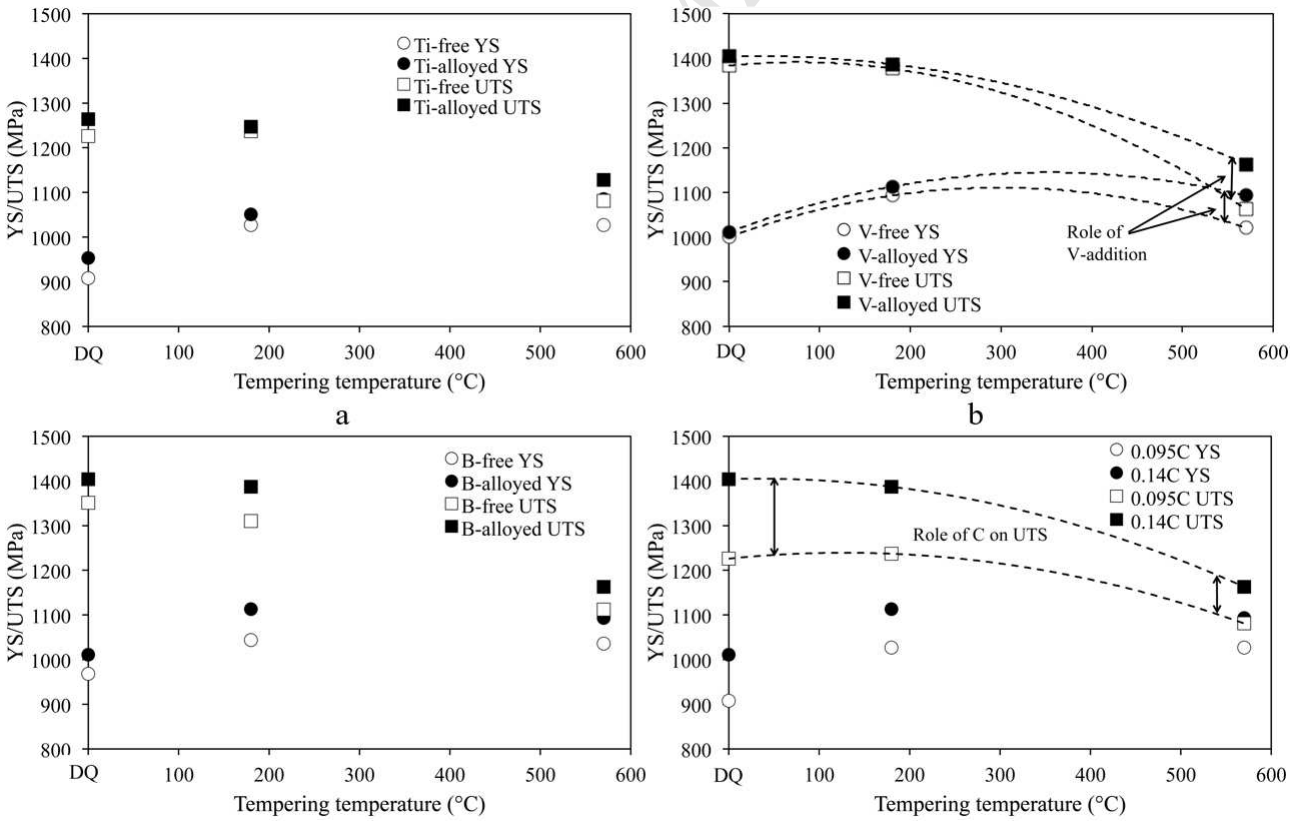

Fig. 13. Effect of titanium (a), vanadium (b), boron (c) and carbon (d) additions on the tensile strength of experimental steels in different tempering conditions. V-addition improves tempering resistance of direct-quenched strip.

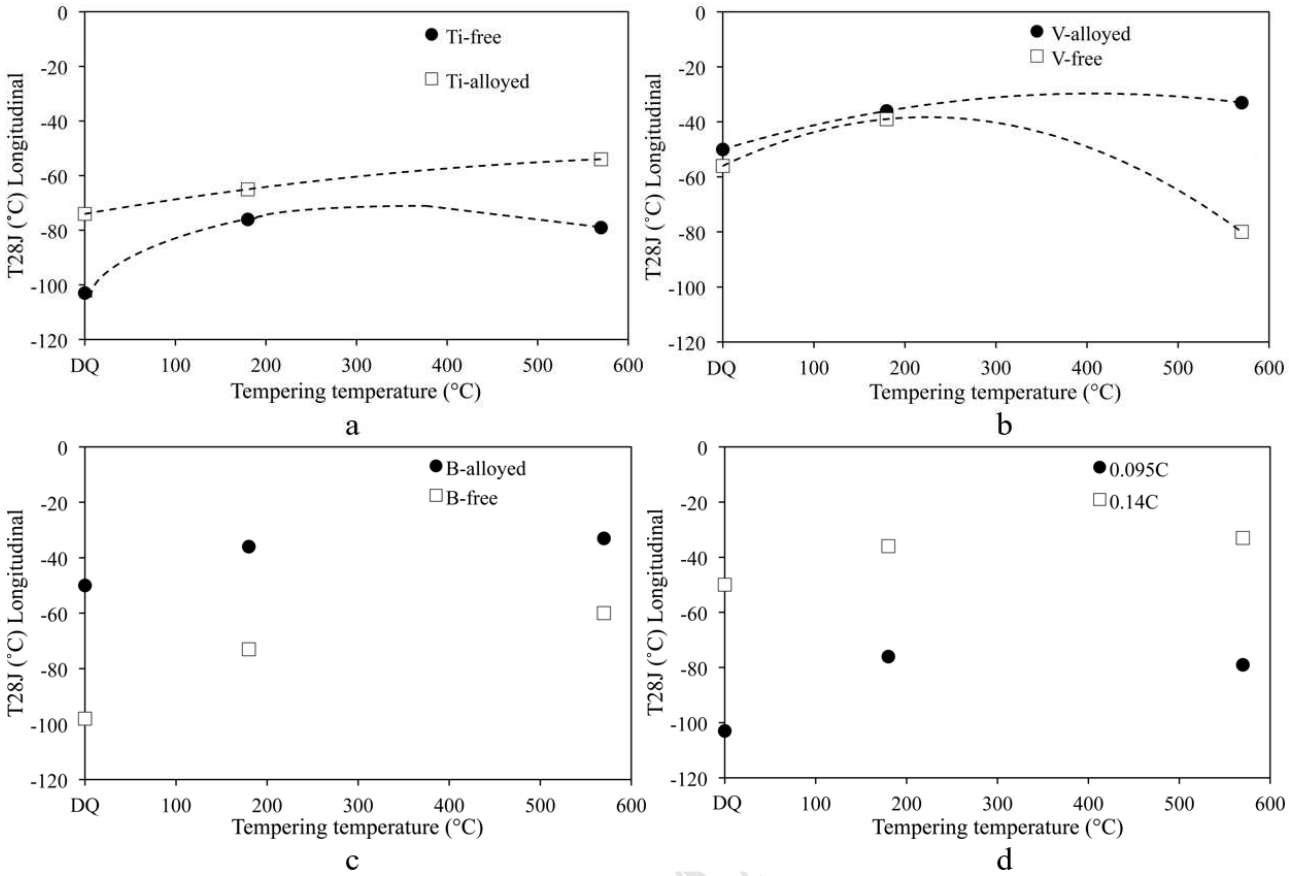

Fig. 14. Effect of titanium (a), vanadium (b), boron (c) and carbon (d) additions on the 28J transition temperature of experimental steels in different tempering conditions. Softened V-free steel is the only steel undergoing improvement in toughness in tempering compared to initial DQ condition.

The results presented above show the many routes that are available for obtaining adequate toughness, ductility and strength in the processing of direct-quenched steel. V-alloyed direct-quenched and tempered steel has high strength even after high-temperature tempering. However, the toughness of the experimental steels is decreased significantly by tempering. In fact, the V-free steel is the only material showing an improvement in toughness after HTT. This type of behaviour is unique and shows a fundamental difference between direct-quenched and re-austenized and quenched martensite, where this kind of behaviour has not been reported. The auto-tempering that occurs in the direct quenching of low-C steel seems to be adequate to provide both excellent toughness and strength already in the DQ condition (see also [28], [54]). However, even though there is no improvement in toughness after tempering, the situation is not that simple. In fact, as can be seen in Fig. 15, when comparing toughness at a certain strength level, the tempered condition offers better 28J transition temperature. Surprisingly though, the HTT and LTT conditions show remarkably similar correlations between yield strength and toughness, i.e. LTT is adequate for optimizing strength and toughness for yield strengths above 1000 MPa. Fig. 15 shows also that B-free 0.14C steel obtained superior strength-toughness combination in all direct-quenched conditions and differs from other materials in the data set. For example, 0.095C and Ti-free steel with similar toughness has 60 MPa lower yield strength while 0.14C and V-free steel obtained roughly same yield strength but over 20 °C high T28J. However, tempering removes this advantage of B-free steel in YS-T28J balance.

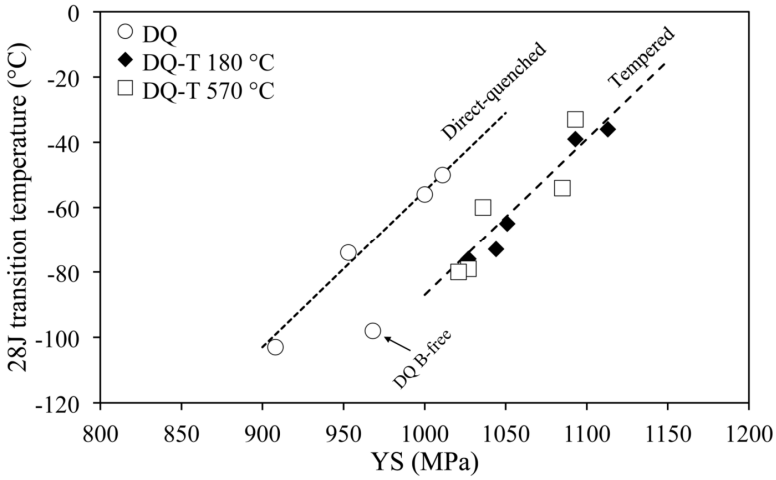

Fig. 15. Effect of yield strength on Charpy V 28 J transition temperature. Dashed lines show the predicted T28J-YS correlation with regression analysis.

The data in Fig. 15 imply that T28J correlates with yield strength and whether or not the material is tempered. Regression analysis of the data resulted the following equation:

$$T28J(°C) = -32.0 \times Tempering + 0.48 \times YS - 535.4 \qquad (1)$$

where *Tempering* is 1 for the HTT and LTT conditions and 0 for the DQ condition and *YS* is yield strength in MPa. R^2 for the equation is 0.93. Fig. 16 shows the goodness of fit of the above equation.

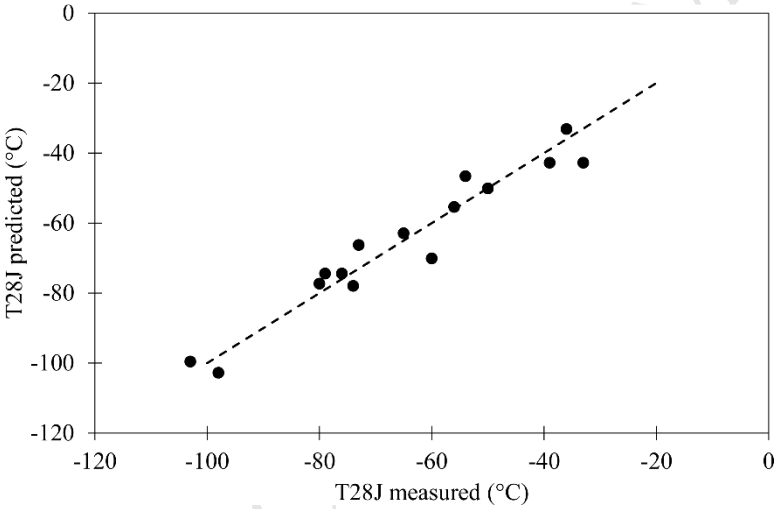

Fig. 16. Correlation between actual T28J and that predicted by Eq. 1.

The regression analysis, as well as YS-T28J plot (Fig. 15) confirms that tempering is beneficial for toughness at a given strength level. For the DQ condition, no material reached the combination of YS 1000 MPa and T28J -75 °C. However, for the HTT condition, it was obtainable using either the low-C V-alloyed Ti-free concept or the high-C V-free concept. For LTT materials on the other hand, the same level of strength and toughness was obtained with the high-C B-free concept and also the low-C V-alloyed composition.

While the two different tempering conditions (LTT and HTT) show remarkable similarities in toughness, greater differences appear in their tensile behaviour. Compared to the DQ and LTT conditions, the HTT condition shows no or very little strain hardening with high yield to tensile

strength ratios (Fig. 13). However, compared to the DQ and LTT conditions both uniform and total elongations are high in the HTT condition. Fig. 17 shows the correlation between strength and both elongation and uniform elongation in the different tempering conditions. The DQ and DQ-LTT conditions follow similar trend lines with an inverse correlation between strength and both A and A_{gt}. DQ-HTT, on the other hand, provides a clearly higher elongation for a given strength level. In fact, total elongation and uniform elongation can be increased in high-temperature tempering making it a suitable option when these ductility parameters are seen as key properties for a particular application. Low-temperature tempering on the other hand does not provide any improvement in total or uniform elongation.

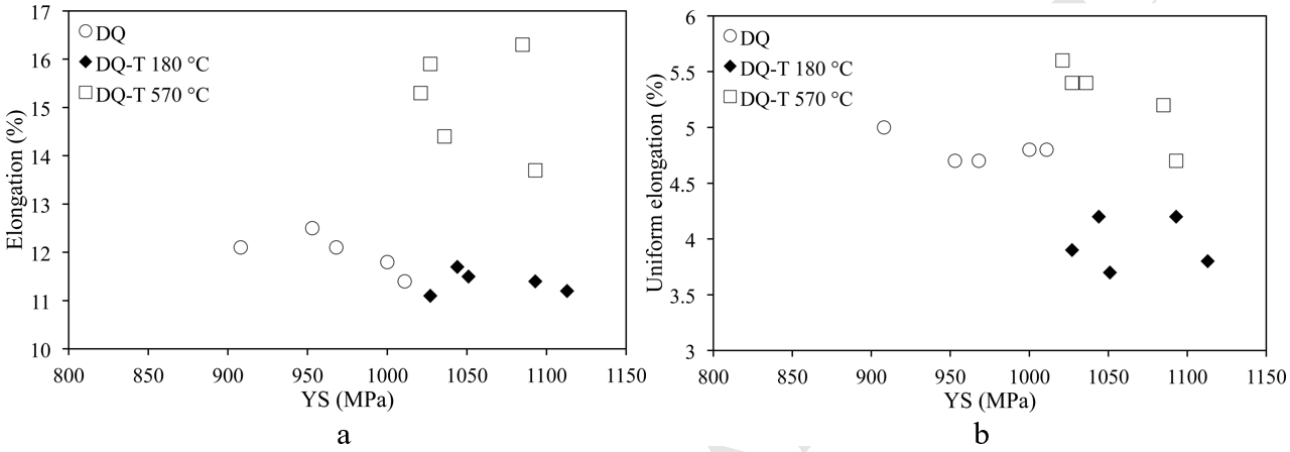

Fig. 17. Total elongation (a) and uniform elongation (b) as a function of yield strength in different tempering conditions.

The results of this study show that careful consideration needs to be given concerning whether the tempering of direct-quenched martensitic and martensitic-ferritic steels is desirable or not. In terms of toughness, no straightforward improvement is obtained with either LTT or HTT treatments with V-alloyed DQ steels. However, when aiming at improved toughness at a certain strength level, which is usually the case, either low-temperature or high-temperature tempering can provide some improvement. Furthermore, if the application demands high strength together with high total and uniform elongation, i.e. tensile ductility, V-alloyed direct-quenched and high-temperature tempered low-C martensite will provide a viable option.

4. CONCLUSIONS

The effects of C (0.095 – 0.14 %), V (0 – 0.08 %), Ti (0 – 0.025 %) and B (0 – 15 ppm) on the microstructure and mechanical properties of direct-quenched and tempered steel with the base composition 0.095C-0.2Si-1.0Mn-1.0Cr-0.65Mo-0.03Al have been studied for low (180 °C) and high (570 °C) tempering temperatures with the aim of finding optimal chemical compositions for retaining strength during the simulated tempering of large steel coils in a bell furnace. Direct quenching nearly 100 °C/s after thermomechanical rolling with a finish rolling temperature of 800 °C produced microstructures containing either 100 % martensite or mixtures of martensite with up to 12 % polygonal ferrite depending on the steel composition. Yield strengths ranged from 900 to 1100 MPa and Charpy V 28 J transition temperatures from -36 to -103 °C. The following conclusions can be drawn:

(1) The addition of 0.08 wt.% V plays an important role in retaining and even increasing strength during high-temperature tempering, but this occurs at the expense of an increase in the Charpy V 28 J transition temperature.
(2) The micro-addition of titanium refined the prior austenite grain structure by controlling austenite grain growth during slab reheating and by controlling recrystallized grain size during thermomechanical treatment. However, this did not lead to improved Charpy V toughness.
(3) Increasing the carbon content had a significant effect on the ultimate tensile strength. This is both due to the higher carbon content of the martensite and a reduction in the volume fraction of polygonal ferrite. Higher carbon content also led to a finer $d_{90\%}$ grain size, but despite this, toughness as measured by T28J was reduced.
(4) Boron is an essential element when aiming at a fully martensitic microstructure in the case of the present compositions and quenching rate. Removing boron from the studied composition led to a mixed microstructure of ferrite and martensite and also finer $d_{90\%}$. Removal of boron also led to significantly increased toughness and superior YS-T28J combination in direct-quenched condition.
(5) Neither high-temperature nor low-temperature tempering improves absolute toughness for the V-alloyed experimental steels, but they both increase toughness at given yield strength level. Both low and high-temperature tempering provide a 30 °C lower transition temperature at a desired level of yield strength.
(6) High-temperature tempered provides significant improvements in tensile ductility without compromising yield strength with V-alloying.
(7) LTT at 180 ˚C leads to a significant increase in yield strength with no loss in the ultimate tensile strength compared to the initial direct-quenched condition due to static aging behaviour. However, this comes with at the expense of toughness and minor decrease in tensile ductility.

ACKNOWLEDGEMENTS

This paper is based on work made within the program “Breakthrough Steels and Applications” of the Digital, Internet, Materials & Engineering Co-Creation, DIMECC Oy. The financial support of SSAB Europe Oy, The Finnish Funding Agency for Technology and Innovation (Tekes) and Jenny and Antti Wihuri foundation is gratefully acknowledged.

Funding: This work was supported by the Finnish Funding Agency for Technology and Innovation (Tekes), SSAB Europe Oy and Jenny and Antti Wihuri foundation.

DATA AVAILABILITY

The raw/processed data required to reproduce these findings cannot be shared at this time as the data also forms part of an ongoing study.

REFERENCES

[1] G. Krauss, “Tempering of Lath Martensite in Low and Medium Carbon Steels: Assessment and Challenges,” *Steel Res. Int.*, vol. 88, no. 10, pp. 1–18, 2017.

[2] G. Krauss and D. K. Matlock, “Effects of Strain Hardening and Fine Structure on Strength and Toughness of Tempered Martensite in Carbon Steels,” *J. Phys. IV*, vol. 5, pp. 51–59, 1995.

[3] G. Krauss, “Martensite in steel: strength and structure,” *Mater. Sci. Eng. A*, vol. 273–275, pp. 40–57, 1999.

[4] R. N. Caron and G. Krauss, “The tempering of Fe-C lath martensite,” *Metall. Trans.*, vol. 3, no. 9, pp. 2381–2389, 1972.

[5] E. I. Galindo-Nava and P. E. J. Rivera-Díaz-Del-Castillo, “A model for the microstructure behaviour and strength evolution in lath martensite,” *Acta Mater.*, vol. 98, 2015.

[6] J. Kömi, P. Karjalainen, and D. Porter, “Direct-Quenched Structural Steels,” in *Encyclopedia of Iron, Steel and Their Alloys*, R. Colás and G. E. Totten, Eds. Boca Raton: CRC Press, 2016, pp. 1109–1125.

[7] A. J. Kaijalainen, P. P. Suikkanen, T. J. Limnell, L. P. Karjalainen, J. I. Kömi, and D. A. Porter, “Effect of austenite grain structure on the strength and toughness of direct-quenched martensite,” *J. Alloys Compd.*, vol. 577, pp. S642–S648, 2013.

[8] H.-W. Yen, M.-H. Chiang, Y.-C. Lin, D. Chen, C.-Y. Huang, and H.-C. Lin, “High-Temperature Tempered Martensite Embrittlement in Quenched-and-Tempered Offshore Steels,” *Metals (Basel).*, vol. 7, no. 7, p. 253, 2017.

[9] C. S. Roberts, B. L. Averbach, and M. Cohen, “The mechanism and kinetics of the 1st stage of tempering,” *Trans. Am. Soc. Met.*, vol. 45, pp. 576–604, 1953.

[10] G. Krauss, “Tempering of Lath Martensite in Low and Medium Carbon Steels: Assessment and Challenges,” *Steel Research International*, vol. 88, no. 10. 2017.

[11] H. K. D. H. Bhadeshia and R. Honeycombe, “The tempering of martensite,” *Steels (Third Ed.*, pp. 183–208, 2006.

[12] S. Morito, J. Nishikawa, and T. Maki, “Dislocation Density within Lath Martensite in Fe–C and Fe–Ni Alloys,” *ISIJ Int.*, vol. 43, no. 9, pp. 1475–1477, 2003.

[13] A. Kaijalainen, S. Pallaspuro, and D. a. Porter, “Tempering of Direct Quenched Low-Alloy Ultra-High-Strength Steel, Part I – Microstructure,” *Adv. Mater. Res.*, vol. 922, pp. 316–321, 2014.

[14] A. Saastamoinen, A. Kaijalainen, D. Porter, P. Suikkanen, J.-R. Yang, and Y.-T. Tsai, “The effect of finish rolling temperature and tempering on the microstructure, mechanical properties and dislocation density of direct-quenched steel,” *Mater. Charact.*, vol. 139, pp. 1–10, Feb. 2018.

[15] H. Li, S. Gao, Y. Tian, D. Terada, A. Shibata, and N. Tsuji, “Influence of Tempering on Mechanical Properties of Ferrite and Martensite Dual Phase Steel,” *Mater. Today Proc.*, vol. 2, no. 0, pp. S667–S671, 2015.

[16] A. Saastamoinen, A. Kaijalainen, D. Porter, and P. Suikkanen, “The effect of thermomechanical treatment and tempering on the subsurface microstructure and bendability of direct-quenched low-carbon strip steel,” *Mater. Charact.*, vol. 134, pp. 172–181, 2017.

[17] W. Yan, Y. Y. Shan, and K. Yang, “Effect of TiN inclusions on the impact toughness of low-carbon microalloyed steels,” *Metall. Mater. Trans. A*, vol. 37, no. 7, pp. 2147–2158, 2006.

[18] S. C. Wang, “The effect of titanium and nitrogen contents on the austenite grain coarsening temperature,” *J. Mater. Sci.*, vol. 24, no. 1, pp. 105–109, 1989.

[19] T. N. Baker, *Titanium technology in microalloyed steels: proceedings of a conference held at the University of Sheffield, December 1994*. Institute of Materials, 1997.

[20] A. Saastamoinen, A. Kaijalainen, D. Porter, and P. Suikkanen, “Effect of titanium and

nitrogen content on the microstructure, hardenability and mechanical properties of direct quenched and tempered ultra-high strength structural steel," in *TMP 2016 - 5th International Conference on ThermoMechanical Processing, Advance Programme*, 2016.

[21] D. Li, F. Huang, S. Wang, Y. Xiong, and S. Xing, "Effect of tempering temperature on microstructures and properties of niobium and titanium microalloying low carbon bainite steel," *Proc. 2nd Int. Conf. Electron. Mech. Eng. Inf. Technol.*, pp. 1542–1545, 2012.

[22] Y. Shen and S. S. Hansen, "Effect of the Ti/N ratio on the hardenability and mechanical properties of a quenched-and-tempered C-Mn-B steel," *Metall. Mater. Trans. A*, vol. 28, no. 10, pp. 2027–2035, 1997.

[23] J. Pacyna and R. Dabrowski, "Vanadium influence upon changes at tempering steels of small content of other elements," *J. Mater. Process. Technol.*, vol. 175, pp. 330–333, 2006.

[24] K. A. Taylor and S. S. Hansen, "The boron hardenability effect in thermomechanically processed, direct-quenched 0.2 Pct C steels," *Metall. Trans. A*, vol. 21, no. 6, pp. 1697–1708, 1990.

[25] J. Hannula *et al.*, "Effect of Boron on the Strength and Toughness of Direct-Quenched Low-Carbon Niobium Bearing Ultra-High-Strength Martensitic Steel," *Metall. Mater. Trans. A*, vol. 48, no. 11, pp. 5344–5356, 2017.

[26] A. Saastamoinen, D. A. Porter, and P. P. Suikkanen, "The microstructure and properties of direct quenched martensite subjected to both slow furnace tempering and rapid induction tempering cycles," in *9th International ROLLING Conference & 6th European ROLLING Conference*, 2013.

[27] T. Kunitake, "Prediction of Ac1, Ac3 and Ms temperatures of by empirical formulas," *J. Japan Soc. Heat Treat.*, vol. 41, pp. 164–169, 2001.

[28] A. Kaijalainen, "Effect of microstructure on the mechanical properties and bendability of direct-quenched ultrahigh-strength steels," University of Oulu, 2016.

[29] T. Nyyssönen, M. Isakov, P. Peura, and V. T. Kuokkala, "Iterative Determination of the Orientation Relationship Between Austenite and Martensite from a Large Amount of Grain Pair Misorientations," *Metall. Mater. Trans. A Phys. Metall. Mater. Sci.*, vol. 47, no. 6, pp. 2587–2590, 2016.

[30] Sente Software, "Tempering of Steels."

[31] Sente Software, "Tempered Hardness of Martensitic Steels."

[32] W. Oldfield, "Curve fitting impact test data: a statistical procedure," 1975.

[33] M. A. EricksonKirk, M. T. EricksonKirk, S. Rosinski, and J. Spanner, "A Comparison of the tanh and Exponential Fitting Methods for Charpy V-Notch Energy Data," *J. Press. Vessel Technol.*, vol. 131, no. 3, pp. 31404–31413, Apr. 2009.

[34] K. Wallin, "Mini- ja normaalikokoisten Charpy-V-koesauvojen tulosten välinen korrelaatio," *VTT Res. reports 428*, p. 31, 1986.

[35] K. Wallin, *Fracture Toughness of Engineering Materials by Kim Wallin, Fracture Toughness of Engineering Materials*. 2011.

[36] F. Nakasato and M. Takahashi, "Effects of boron, titanium, and nitrogen on the hardenability of boron-treated steels for heavy machinery," *Met. Technol.*, vol. 6, no. 1, pp. 102–105, 1979.

[37] H. Adrian and F. B. Pickering, "Effect of titanium additions on austenite grain growth kinetics of medium carbon V–Nb steels containing 0·008–0·018%N," *Mater. Sci. Technol.*, vol. 7, no. 2, pp. 176–182, 1991.

[38] V. Blancas-garcia and V. Blancas-garcia, "A NEW VIEW OF THE GRAIN-COARSENING BEHAVIOR OF AUSTENITE IN TI-MICROALLOYED LOW-CARBON STEELS," University of Pittsburgh, 2016.

[39] B. Feng, "Effect of Ti and Ti-Nb on the stability of the austenite grain structure and [austenite to ferrite] transformation characteristics in C-Mn steel under hot rolling conditions," University of Wollongong, 1991.

[40] S. F. Medina, M. I. Vega, and M. Gómez, "Influence of TiN Particles on Dynamic and Static

Recrystallization in Microalloyed Steels," *Mater. Sci. Forum*, vol. 467, pp. 1205–1210, 2004.
[41] H. Kobayashi, "Effect of Vanadium and Niobium on Austenite Grain Growth Kinetics in Low Carbon High Strength Steel," *Tetsu-to-Hagane*, vol. 63, no. 1, pp. 73–79, 1977.
[42] A. J. Kaijalainen, P. Suikkanen, L. P. Karjalainen, and J. J. Jonas, "Effect of Austenite Pancaking on the Microstructure, Texture, and Bendability of an Ultrahigh-Strength Strip Steel," *Metall. Mater. Trans. A*, vol. 45, no. 3, pp. 1273–1283, Mar. 2014.
[43] S. Pallaspuro, A. Kaijalainen, S. Mehtonen, J. Kömi, Z. Zhang, and D. Porter, "Effect of microstructure on the impact toughness transition temperature of direct-quenched steels," *Mater. Sci. Eng. A*, vol. 712, no. December 2017, pp. 671–680, 2018.
[44] Y. Gao, X. Xue, and H. Yang, "Influence of Boron on Initial Austenite Grain Size and Hot Deformation Behavior of Boron Microalloyed Steels," pp. 592–607, 2015.
[45] A. Bag, K. K. Ray, and E. S. Dwarakadasa, "Influence of martensite content and morphology on tensile and impact properties of high-martensite dual-phase steels," *Metall. Mater. Trans. A*, vol. 30, no. 5, pp. 1193–1202, 1999.
[46] P. P. Suikkanen *et al.*, "Effects of Carbon Content and Cooling Path on the Microstructure and Properties of TRIP-aided Ultra-High Strength Steels," *ISIJ Int.*, vol. 53, no. 2, pp. 337–346, 2013.
[47] B. Hutchinson, D. Lindell, and M. Barnett, "Yielding Behaviour of Martensite in Steel," *ISIJ Int.*, vol. 55, no. 5, pp. 1114–1122, 2015.
[48] D. Lohe and V. O., *Stability of residual stresses, Handb. Residual Stress Deform. Steel*. 2002.
[49] G. F. Harvey, "MATHEMATICAL SIMULATION OF TIGHT COIL ANNEALING.," vol. 22, pp. 28–37, 1977.
[50] R. Lagneborg, T. Siwecki, S. Zajac, and B. Hutchinson, "The Role of Vanadium in Microalloyed Steels," *Scand. J. Metall.*, vol. 28, no. October, pp. 186–241, 1999.
[51] S. Gündüz and R. C. Cochrane, "Influence of cooling rate and tempering on precipitation and hardness of vanadium microalloyed steel," *Mater. Des.*, vol. 26, pp. 486–492, 2005.
[52] S. Fukui, N. Uehara, and K. Isokawa, "The Effect of Vanadium on the Hardenability and Mechanical Properties of High Strength Steels," *DENKI-SEIKO[ELECTRIC Furn. STEEL]*, vol. 42, no. 4, pp. 272–287, 1971.
[53] H. Adrian, "A mechanism for effect of vanadium on hardenability of medium carbon manganese steel," *Mater. Sci. Technol.*, vol. 15, no. 4, pp. 366–378, 2013.
[54] S. Pallaspuro, "On the factors affecting the ductile-brittle transition in as-quenched fully and partially martensitic low-carbon steels," University of Oulu, 2018.

Article reference: MSA_MSEA-D-19-01923

Article title: Direct-quenched and tempered Low-C high-strength structural steel:The role of chemical composition on microstructure and mechanical properties

Corresponding author:
M.Sc. Ari Saastamoinen (ari.saastamoinen@tuni.fi)

Affiliation: Tampere University, Materials Science. Centre for Advanced Steels Research. 33720 Tampere, Finland

Other authors:
Dr. Antti Kaijalainen (antti.kaijalainen@oulu.fi), B.Sc. Tun Tun Nyo (tunnyo@oulu.fi), Dr. David Porter (david.porter@oulu.fi), Dr. Jukka Kömi (jukka.komi@oulu.fi)

Affiliation: University of Oulu, Centre for Advanced Steels Research. PL 8000, 90014 Oulu, Finland

Dr. Pasi Suikkanen (pasi.suikkanen@ssab.com)

Affiliation: SSAB Europe Oy. Rautaruukintie 155, 92100 Raahe